



## The morphology and mechanical properties of $Zr_{59}Nb_5Cu_{18}Ni_8Al_{10}$ metallic glasses

Badis Bendjemil<sup>1,2,3,\*</sup>, Ali Hafs<sup>1</sup>, Nassima Seghairi<sup>4</sup>, Marcello Baricco<sup>2</sup>

<sup>1</sup>LEREC, University of Badji Mokhtar, P. Box 12, 23000 Annaba, Algeria

<sup>2</sup>Università di Torino, Via P. Giuria 9, 10125 Torino, Italy

<sup>3</sup>University of 08 mai 1945, P. Box 401, 24000 Guelma, Algeria

<sup>4</sup>University of Oum El-Bouaghi, 04000 Oum El-Bouaghi, Algeria

Received 23 April 2011; Revised 24 June 2011; Accepted 28 July 2011

### Abstract

In the present work, the glass formation of  $Zr_{59}Nb_5Cu_{18}Ni_8Al_{10}$  alloys of 2 mm diameter were prepared through casting in water cooled copper mould and in a ribbon form by the single roller melt spinning method. This study is primarily devoted to evaluate the results obtained by the two methods. The thermal stability was evaluated by differential scanning calorimetry (DSC) at a heating rate of 10 °C/mn. The glass formation, structural properties and morphology of the bulk metallic glass are presented, including glass transition temperature ( $T_g$ ) and crystallization temperature ( $T_x$ ). The microstructure and phases composition of the alloy have been analyzed using X-ray diffraction and indicate that the alloy is fully amorphous. The mechanical properties of bulk  $Zr_{59}Nb_5Cu_{18}Ni_8Al_{10}$  alloy is obtained by compression tests at room temperature. The fracture and morphologies after compression test are observed by Scanning Electron Microscopy (SEM), revealed the fragile plastic of the alloy. The Energy Dispersive Spectrometer (EDS) micro-analysis is performed by measuring the energy and intensity distribution of X-ray signals generated by a focused electron beam on the specimen with a diameter 2 mm.

**Keywords:** Bulk metallic glasses; Amorphous phase; XRD.

**PACS:** 81.20.Ka; 74.70.-b; 75.50.-y.

### 1. Introduction

Amorphous alloys, also known as metallic glasses, have attracted intense scientific and technological attention since amorphous metal was first discovered [1]. Due to the lack of defects such as grain boundaries and dislocations, amorphous alloys exhibit extraordinary properties including superior mechanical properties and lower thermal conductivity as well as extreme wear and corrosion resistance. Amorphous alloys are therefore considered to be promising structural as functional materials for practical applications. However, the critical cooling rate typically required is above  $10^6$  K/s, for retaining the metastable amorphous phase during cooling process. Consequently, the size of the amorphous alloys obtained was limited to thin ribbons, tiny wires and small powders. This strongly restricts the further applications of the amorphization techniques.

---

\*) For correspondence : Tel : 06972804756, E-mail : [bendjemilbadis@yahoo.fr](mailto:bendjemilbadis@yahoo.fr).

Since the late 1980s, investigations of multi-component liquid alloys with very deep eutectics have led to the development of metallic glasses with high glass-forming ability (GFA). The development of these metal alloys enables the fabrication of glassy samples with a thickness greater than 1mm, which is known as bulk metallic glasses (BMGs).

This development makes the application of BMGs, particularly Zr-based bulk metallic glasses, have drawn much attention as new materials, which possess useful engineering properties such as high-mechanical strength, good ductility, and high-corrosion resistance [2, 3, 4]. Recently, many kinds of BMGs have been discovered and investigated in various alloy systems such as  $Zr_{65}Nb_5Cu_{12.5}Ni_{10}Al_{7.5}$  [5],  $Zr_{55}Cu_{25}Ni_5Al_{10}Nb_5$  [6],  $Zr_{58}Al_9Ni_9Cu_{14}Nb_{10}$  [7],  $Zr_{60}Nb_xCu_{22-x}Ni_{10}Al_{10}$  ( $x=0-15$ ) [8],  $Zr_{66.4}Nb_{6.4}Al_{18}Ni_{8.7}Cu_{10}$  [9],  $Zr_{65}(Cu_{0.4}Al_{0.3}Ni_{0.3})_{28}Nb_7$  [10]. The cooling rate for these BMGs varies in the range of  $10^{-1}$  to  $10^3$  K/s with a range of difference between the quenching rates of the bulk and ribbon metal glasses, a window of opportunity becomes available for the investigation of glasses with the same composition but produced in various structural states.

The aim of the present work is to study the behaviour of glass formation of the  $Zr_{59}Nb_5Cu_{18}Ni_8Al_{10}$  prepared by the melt-spinning process, in the ribbon shape, and then injected into a copper mould to prepare alloy rods of about 2 mm in diameter. The mechanical properties of the composite have been examined through compression tests and indentation fracture of amorphous alloy is presented.

## 2. Experimental

An ingot of the  $Zr_{59}Ti_5Cu_{18}Ni_8Al_{10}$  alloy (composition is given in nominal atomic %) of Zr 99.99 mass% purity, Nb 99.8 mass%, Cu 99.9 mass%, Ni 99.9 mass% and Al 99.9 mass% purity mixtures in an argon atmosphere was prepared using the casting by injection into a water-cooled copper mould with the form of 50 mm long cylinder with diameter of 2 mm. For comparison, the ribbon with 5 mm width and about 30  $\mu$ m thickness was prepared using a single roller, melt spinning technique under a vacuum atmosphere.

All the ribbons and cylinders were investigated by differential scanning calorimetry (DSC) using a constant heating rate of 10°C/mn. The structural properties of the samples were examined by X-ray diffraction (XRD) with Cu K $\alpha$  ( $\lambda = 1.54056 \text{ \AA}$ ) radiation. Scanning electron microscopy (JEOL JSM6400F) was employed for the analysis of the fracture features after compression test. The mechanical properties were tested using an Instron testing machine at a strain rate of  $5 \times 10^{-4} \text{ s}^{-1}$  at room temperature.

## 3. Results and discussion

Fig. 1 shows comparably two DSC curves. One is obtained from a melt-spun  $Zr_{59}Nb_5Cu_{18}Ni_8Al_{10}$  glass ribbon and another from the rod with a diameter of 2 mm. The results in Fig. 1 shows the constant rate heating (10 °C/mn) DSC curves of  $Zr_{59}Nb_5Cu_{18}Ni_8Al_{10}$  analysis was carried out for melt-spun ribbons and as-cast cylinders. In the temperature range investigated, all the curves are characterized by two exothermic peaks, revealing a multi-step crystallization path that does not depend on the way of preparation. The analysis of the thermal stability data, summarized in Table 1, reveals striking similarities between the as cast cylinder and the melt spun ribbon.

The DSC curves indicate a small difference in glass transition temperature ( $T_g$ ), crystallization temperature ( $T_x$ ), supercooled liquid region ( $\Delta T_x = T_x - T_g$ ) between the ribbon and rod samples, for the as cast of 2 mm diameter cylinder shows that the ribbon alloy presents two over-lapping exothermic peak around 367 and 601 °C. The glass transition temperature,  $T_g$ , is 333 °C. The melt-spun ribbon for the same alloy presents two

exothermic peaks corresponding to two distinct stages of phase transformations  $T_{x1}$  and  $T_{x2}$  (369 °C and 602 °C, respectively) and an obvious  $T_g = 335^\circ\text{C}$ .

Table 1: Summary of the glass transition temperature  $T_g$ , crystallization temperature  $T_{x1}$ ,  $T_{x2}$ , and supercooled temperature region  $\Delta T_x$  for the melt-spun ribbons and as-cast rod 2 mm (continuous heating at  $10^\circ\text{C}/\text{mn}$ ).

Temperatures	Melt spun ribbon	As cast rod of 2 mm
$T_g$ (°C)	335	333
$T_{x1}$ (°C)	369	367
$T_{x2}$ (°C)	602	601
$\Delta T_x$ (°C)	34	34

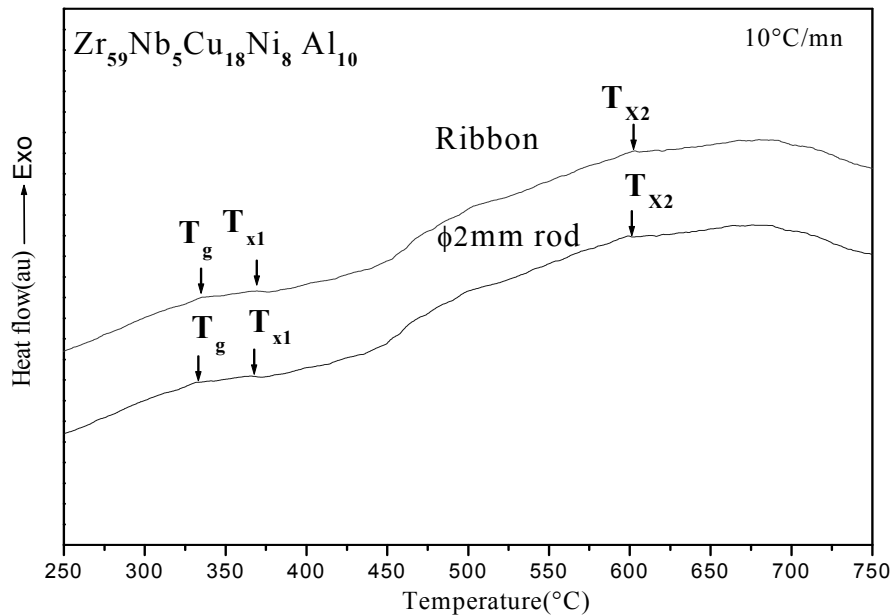


Fig. 1: DSC curves of  $\text{Zr}_{59}\text{Nb}_5\text{Cu}_{18}\text{Ni}_8\text{Al}_{10}$  alloy ribbon and rods with diameters of 2mm.

In order to confirm the glassy state of the samples, further X-ray diffraction measurements were performed. Fig. 2 shows XRD pattern of the cast  $\text{Zr}_{59}\text{Nb}_5\text{Ti}_5\text{Cu}_{18}\text{Ni}_8\text{Al}_{10}$  rod with a diameter of 2 mm, together with the XRD pattern of the melt spun glassy alloy ribbon. Only a broad peak is seen around a diffraction angle of 40 degrees for the bulk sample and ribbon, indicating the formation of a glassy phase.

These are typical XRD patterns of amorphous structures, confirming that both samples possess amorphous structures.

The critical cooling rate for glass formation,  $R_c$ , is an important characteristic parameter for predicting the ease or difficulty of glass formability. It is defined as the minimum cooling rate necessary to keep the melt amorphous without detectable crystallization upon solidification. A slower  $R_c$  indicates a greater glass-forming ability of an alloy system.

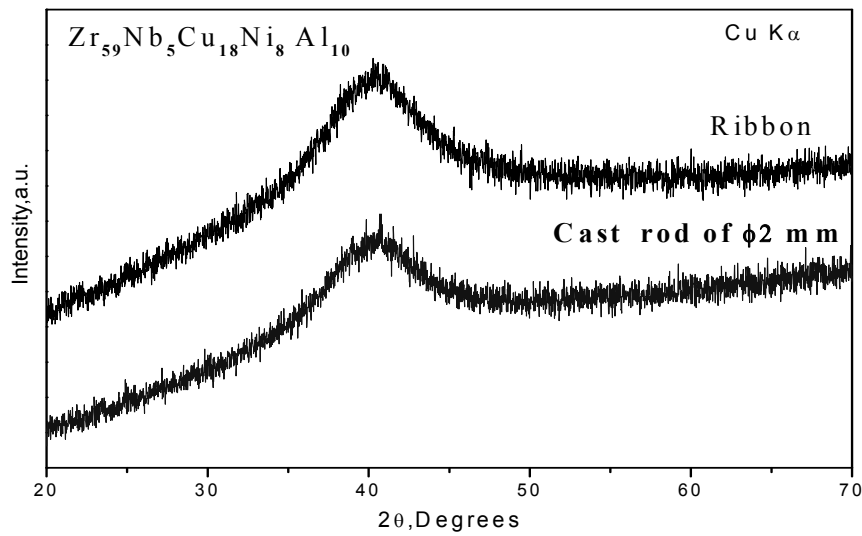


Fig. 2: XRD pattern of the cast  $Zr_{59}Nb_5Cu_{18}Ni_8Al_{10}$  rod with a diameter of 2 mm, together with the XRD pattern of the melt-spun glassy alloy ribbon.

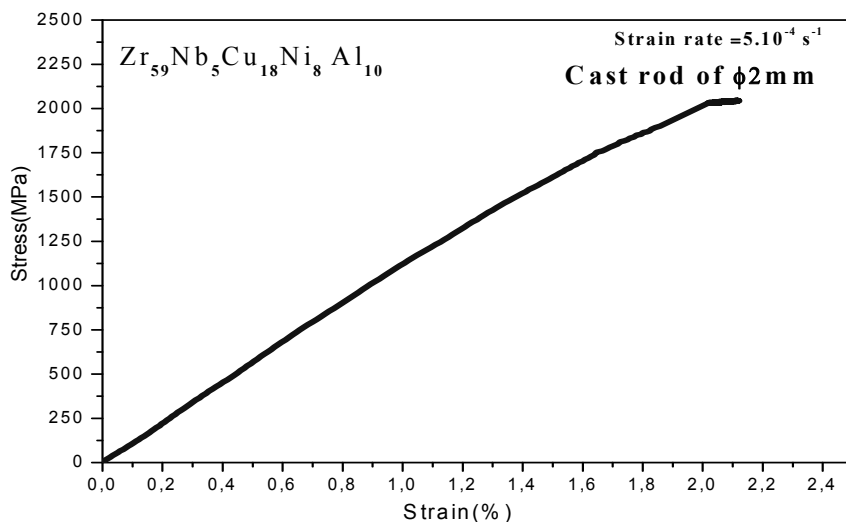


Fig.3: Compressive stress–strain curve of as cast rod  $Zr_{59}Nb_5Cu_{18}Ni_8Al_{10}$  glassy alloy under a uniaxial compression testing at room temperature.

The room temperature compression results are in good agreement with the report. In addition,  $Zr_{59}Nb_5Cu_{18}Ni_8Al_{10}$  alloy shows the compressive stress–strain curve at a strain rate of  $5.10^{-4}\ s^{-1}$  (Fig.3).

The fracture of the samples occurs at a fracture stress  $\sigma_f$  of 2022 MPa and elastic a deformation up to a strain of about 2.02 % followed by a small compressive plastic strain in the range of 2.02 -2.12. The Young’s modulus is determined as 100 GPa for the 2 mm diameter sample, which is larger than those of the

$Zr_{65}Al_{17.5}Ni_{10}Cu_{17.5-x}Ag_x$  ( $x=5$  and  $10$  at %) BMGs, but is comparable to that of the annealed  $Zr_{65}Al_{17.5}Ni_{10}Cu_{12.5}Ag_5$  alloy containing approximately 85% nanometer scaled I-phases [10] and  $Zr_{58}Al_9Ni_9Cu_{14}Nb_{10}$  alloy containing 90% quasicrystal. The elasticity is several times superior than that of  $Al_{63.5}Cu_{24.5}Fe_{12}$  and  $Al_{70}Pd_{20}Mn_{10}$  poly-crystalline

icosahedral quasicrystals [19, 20], while the measured Young's modulus value is much lower than those of the conventional quasicrystals as shown in Table 2.

Table 2: Mechanical properties of the present materials compared with Al- and Zr-based non-crystalline alloys.

Materials	Phase constituents	Elastic stress limit $\sigma_f$ (Mpa)	Elastic deformation limit $\epsilon_e$ (%)	Young's modulus E (GPa)
Al <sub>70</sub> Pd <sub>20</sub> Mn <sub>10</sub> [11]	I-phase	520 (fracture)	0.3	200
Al <sub>63</sub> Cu <sub>25</sub> Fe <sub>12</sub> [12]	I-phase	250 (fracture)	0.35	172 [13]
Zr <sub>65</sub> Al <sub>17.5</sub> Ni <sub>10</sub> Cu <sub>12.5</sub> Ag <sub>5</sub> [14]	BMGs	1650 (fracture)	1.95	84.5
Zr <sub>65</sub> Al <sub>17.5</sub> Ni <sub>10</sub> Cu <sub>12.5</sub> Ag <sub>5</sub> [14]	85% quasicrystal +15% glass	1200 (fracture)	1.5	90
Zr <sub>58</sub> Al <sub>9</sub> Ni <sub>9</sub> Cu <sub>14</sub> Nb <sub>10</sub> [15]	90% quasicrystal +10% glass	1800 (fracture)	2.0	92
Zr <sub>59</sub> Nb <sub>5</sub> Cu <sub>18</sub> Ni <sub>8</sub> Al <sub>10</sub> (this work)	BMGs	2022(fracture)	2.02	100

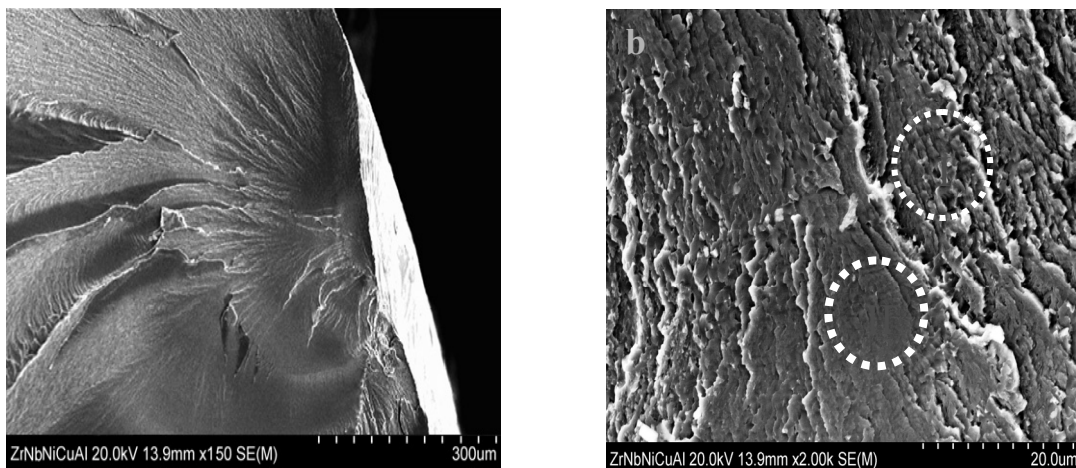


Fig. 4: SEM micrographs of the fracture morphology of Zr<sub>59</sub>Nb<sub>5</sub>Cu<sub>18</sub>Ni<sub>8</sub> Al<sub>10</sub> amorphous rod in as cast state with diameter of 2 mm, (a) low magnification exhibiting the river patterns and (b) the higher magnification images showing the typical characteristics of the fragile fracture.

The SEM observation on the fracture surface of broken samples provides insight into the fracture mechanism of the alloy. Fig. 4 shows the secondary electron images taken for the fractured surface. Rivers like shape are to be composed of a high number and predominate in the fracture surface (Fig. 4a). The fracture surface appears to consist of a high number of small fracture zones, which leads to breaking of the samples into many small parts, as indicated in Fig. 4b. It indicates that the fracture of metallic glasses can occur either in a shear mode or in a break mode, depending on the constituent elements and microstructure in detail. The actual failure mode of a metallic glassy sample is a competition result between shear fracture and distensile fracture as reported by Zhang et al. [16].

Significantly, instead of shattering into multiple pieces, as occurs for most brittle Zr-based BMGs [17, 18], all the BMG composite samples in the present study were fractured into two parts along the main shear band, implying that this material probably also has a good toughness. The fracture surface of the BMG composite displays a mixture of a well-

developed vein pattern as indicated in region I and a relatively smooth area as indicated in region II (see Fig. 4b). Region II was probably caused by the whole slip or movement of a dendrite phase as the glassy matrix softened due to adiabatic heating. Compared to monolithic BMG, the vein patterns in the BMG composite are rather rough (see the inset of Fig. 4b), indicating that the dendrite phase effectively impeded the immediate shear-off and failure during shear band propagation. In order to clarify how the dendrite phase interacts with shear bands and contributes to the enhancement of plasticity, the BMG composite rod was further subjected to a compression test, in which a part of the side surfaces of the rod was first polished to a mirror finish, then compressed to fracture at a strain rate of  $5 \times 10^{-4} \text{ s}^{-1}$  at room temperature

The results of chemical analysis of as cast rod  $\text{Zr}_{59}\text{Nb}_5\text{Cu}_{18}\text{Ni}_8\text{Al}_{10}$  with a diameter of 2 mm by EDS attached to SEM pictures are shown in Fig. 5.

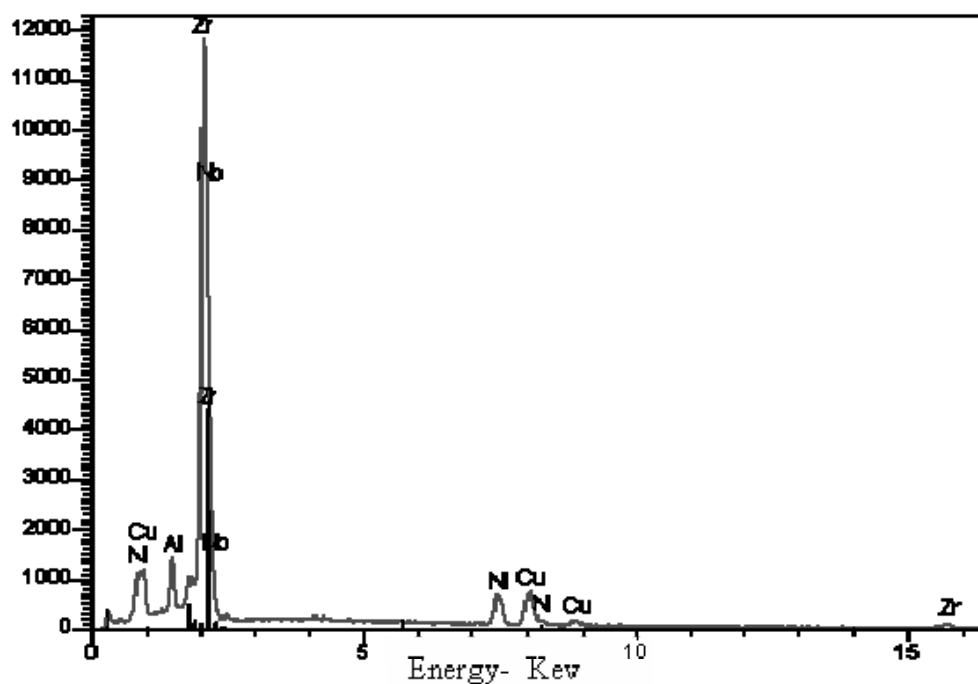


Fig.5: Energy dispersive spectra of the  $\text{Zr}_{59}\text{Nb}_5\text{Cu}_{18}\text{Ni}_8\text{Al}_{10}$  alloy.

#### 4. Conclusion

In conclusion, The comparison between the ribbon were obtained directly from the melt-spinning technique and the same alloy produced by injection casting of the molten alloy into copper mould with cylindrical cavities reveals that both types of samples are characterized by the formation of the amorphous phase confirmed by X-ray diffraction . The bulk glassy rods possess good mechanical properties, the compressive fracture strength and elastic strain to fracture of the amorphous alloy with 2, 02 % also exhibit ultrahigh fracture strength of 2022 MPa and Young's modulus of 100 GPa. The fracture after compression test observed by SEM revealed the fragility of the alloy.

## Acknowledgement

We acknowledge the group of Prof. Dr M. Baricco, Prof. Dr Jamal Bougdira head of the department Jean LAMOUR, Dr Ghouti Madjahdi and Pascal from the Nancy University, France for the synthesis and characterisations of the samples.

## References

- [1] P. Duwez, R. H. Willens, W. Klement, *J. Appl. Phys.* **31** (1960) 1137
- [2] A. Inoue, T. Zhang, *Mater. Trans. JIM* **37** (1996) 185
- [3] A. Inoue, Y. Kawamura, T. Shibata, K. Sasamori, *Mater. Trans. JIM* **37** (1996) 1337
- [4] J. F. Hoffler, *Intermetallics* **11** (2003) 529
- [5] J. Saida, A. Inoue, *Journal of non-crystalline solids* **312-314** (2002) 502
- [6] Q. Wang, J. M. Pelletier, L. Xia, H. Xu, Y. D. Dong. *Journal of Alloys and Compounds* **413** (2006) 181
- [7] J. B. Qiang, W. Zhang, Guoqiang Xie, Hisamichi Kimura, C. Dong, A. Inoue. *Intermetallics* **15** (2007) 1197e1201
- [8] F. Cang, A. Inoue. *Scripta Materialia* **45** (2001) 115
- [9] U. Kühn, J. Eckert, N. Mattern, L. Schultz. *Materials Science and Engineering A* **375–377** (2004) 322
- [10] H. Yongjiang, S. Jianfei, Y. Xin, S. Jun. *Rare Metal Materials and Engineering*, **37** 3 (2008) 0391
- [11] Y. Yokoyama, A. Inoue Masumoto T. *Mater Trans JIM* **34** (1993) 135
- [12] U. Koster, H. Liebertz W. Liu, *Mater Sci Eng A* **777** (1994) 181e182
- [13] J. J. Vanderwal, P. Zhao, D. Walton. *Phys Rev*, **B46** (1992) 501
- [14] Inoue A. Zhang T. Chen M. W, Sakurai T. *Mater Trans JIM*, **40** (1999) 1382
- [15] J. B. Qiang, W. Zhang, Guoqiang Xie, Hisamichi Kimura, C. Dong, A. Inoue. *Intermetallics* **15** (2007) 1197e1201
- [16] Z. F. Zhang, G. He, J. Eckert, L. Schultz, *Phys. Rev. Lett.* **91** (2003) 045505
- [17] Q. J. Chen, J. Shen, D. L. Zhang, H. B. Fan, J. F. Sun, *J. Mater. Res.* **22** (2007) 358
- [18] F. F. Wu, Z. F. Zhang, B. L. Shen, S. X. Mao, J. Eckert, *Adv. Eng. Mater.* **10** (2008) 727

